



Short communication

## Synthesis and molecular modelling studies of novel sulphonamide derivatives as dengue virus 2 protease inhibitors



Ajay Kumar Timiri<sup>a</sup>, Selvarasu Subasri<sup>b</sup>, Manish Kesharwani<sup>b</sup>, Vijayan Vishwanathan<sup>b</sup>,  
Barij Nayan Sinha<sup>a</sup>, Devadasan Velmurugan<sup>b</sup>, Venkatesan Jayaprakash<sup>a,\*</sup>

<sup>a</sup> Department of Pharmaceutical Sciences and Technology, Birla Institute of Technology, Mesra, Ranchi 835215, Jharkhand, India

<sup>b</sup> Centre for Advanced Study in Crystallography and Biophysics, University of Madras, Chennai 600 025, Tamil Nadu, India

## ARTICLE INFO

## Article history:

Received 15 May 2015

Revised 27 July 2015

Accepted 28 July 2015

Available online 29 July 2015

## Keywords:

Antiviral

Dengue

NS2B–NS3 protease

Phthalimide

Sulphonamides

Molecular docking

Molecular interactions

## ABSTRACT

Development of antivirals for dengue is now based on rational approach targeting the enzymes involved in its life cycle. Among the targets available for inhibition of dengue virus, non-structural protein NS2B–NS3 protease is considered as a promising target for the development of anti-dengue agents. In the current study we have synthesized a series of 4-(1,3-dioxo-2,3-dihydro-1H-isoindol-2-yl)benzene-1-sulphonamide derivatives and screened for DENV2 protease activity. Compounds **16** and **19** showed IC<sub>50</sub> of DENV2 Protease activity with 48.2 and 121.9 μM respectively. Molecular docking and molecular dynamic simulation studies were carried out to know the binding mode responsible for the activity. MD simulations revealed that, NS2B/NS3 protease was more stable when it binds with the active compound. Structure optimization of the lead compounds **16** and **19** and their co-crystallization studies are underway.

© 2015 Elsevier Inc. All rights reserved.

### 1. Introduction

Dengue is the oldest viral infection reported in Chinese medical encyclopedia during the Jin-dynasty (265–420 AD) as “water poison” associated with flying insects [1]. First confirmed case of dengue case reported in 1789 and is by Benjamin Rush, who coined the term “break bone fever” because of the symptoms of myalgia and arthralgia [2]. Dengue is widespread mosquito-borne disease, which is rapidly spreading throughout the globe where the mosquito vector *Aedes aegypti* is found [3]. Dengue infection is caused by dengue virus (DENV), which belongs to the family Flaviviridae [4] and is one of the major emerging pathogens for which there is neither a vaccine nor any antiviral therapy. Among all viral hemorrhagic fevers, dengue accounts maximum [5]. There are four serotypes in Dengue virus, DENV1–DENV4 [6]. According to World Health Organization (WHO) statistics 2012, 2.5 billion people are at risk for dengue infection throughout the world [7]. A recent study estimates about 390 million dengue infections takes per year, in which 96 million manifest some level of clinical or subclinical severity [8]. Another study estimates that 3900 million in 128 countries are at risk with dengue virus [9]. Dengue virus has RNA as genetic material. Upon infection, the genomic RNA of the virus

is translated by the host cell machinery into a single polyprotein, which is subsequently cleaved and processed into ten distinct structural (C, prM and E) and nonstructural (NS1, NS2A, NS2B, NS3, NS4A, NS4B and NS5) proteins [6]. Dengue Virus encodes for a two component protease NS2B–NS3 which is responsible for the processing at the junctions of NS2A/NS2B, NS2B/NS3, NS3/NS4A and NS4B/NS5, as well as at internal sites within C, 2A, NS3, NS4A [6,10,11]. This makes the NS2B–NS3 protease an ideal target for drug design against dengue infection.

Non-peptidic small molecule inhibitors are targeted successfully against HCV and HIV viral proteases and their resistant strains [12–14]. Moreover, small molecule inhibitors promote large conformational changes in the dengue virus NS2B–NS3 protease [15] for example, 8-hydroxy quinoline derivatives [16], anthracene based inhibitors [17], α-keto amides [18], aryl cyanoacryl amides [19], 1,2-benzisothiazole-3(2H)-one, 1,3,4-oxadiazole hybrid derivatives [20], benz[d]isothiazol-3(2H)-one derivatives [21] and cyclohexenylchalcone derivatives from natural product [22]. They were reported to inhibit DENV protease.

High throughput virtual screening (HTVS) protocol was found very successful for getting leads in drug discovery [23]. In an attempt to obtain selective inhibitors of the DENV NS2B/NS3 protease, HTVS was performed. Whole Zinc 8 database was filtered for drug like molecules and resultant dataset was docked to DENV2 NS2B/NS3 protease (pdb code: 2FOM [24]). Top hundred

\* Corresponding author.

E-mail address: [venkatesanj@bitmesra.ac.in](mailto:venkatesanj@bitmesra.ac.in) (V. Jayaprakash).

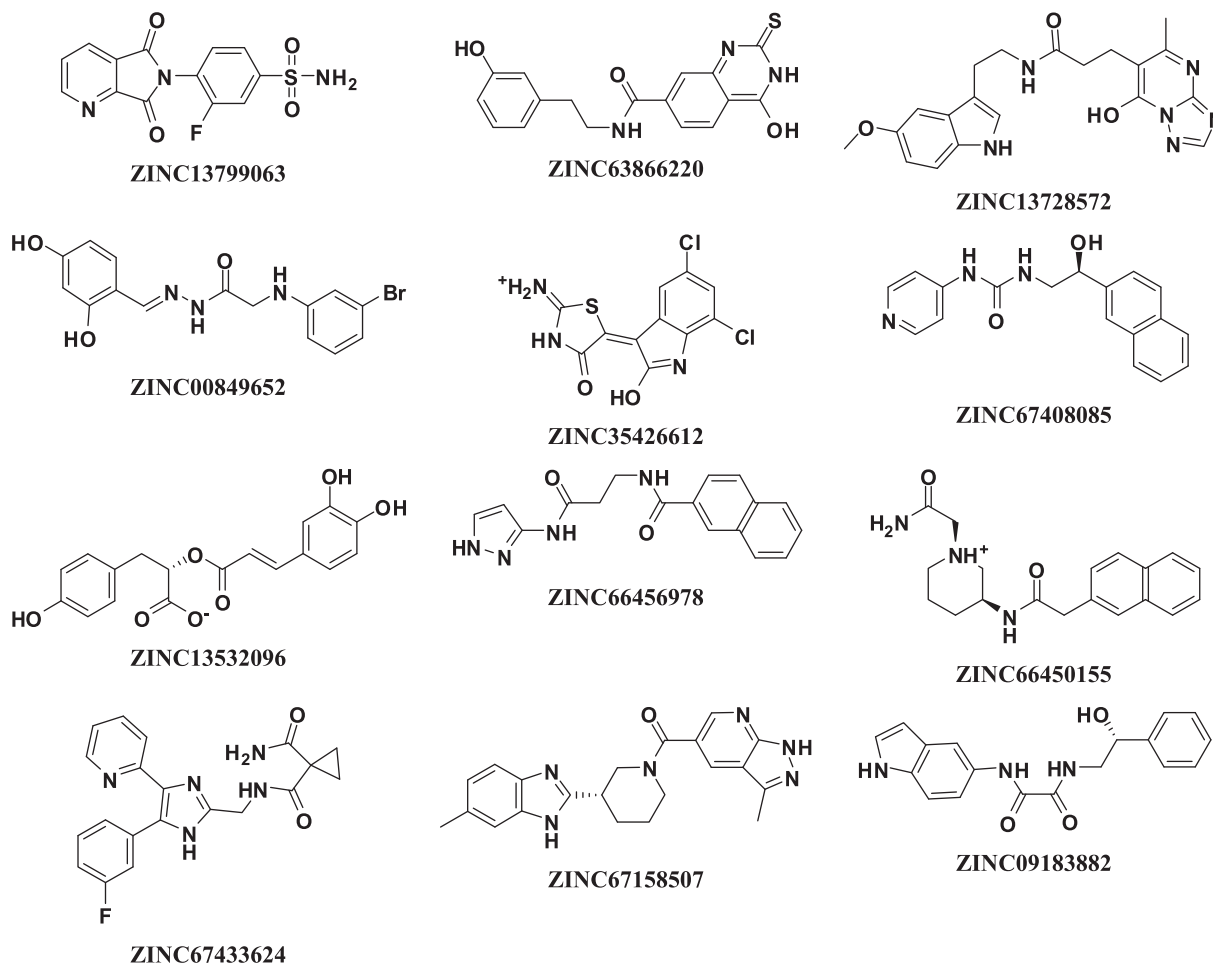


Fig. 1. Best scaffolds as inhibitors against DENV2 protease.

**Table 1**  
DENV protease activity of Compounds 1–20.

1-18

Compound code	R	R <sup>1</sup>	IC <sub>50</sub> (μM)
1	H	H	>100
2	Methyl	Methyl	>100
3	Ethyl	Ethyl	>100
4	Isopropyl	H	>100
5			>100
6			>100
7	Phenyl	H	>100
8	2-Hydroxy Phenyl	H	>100
9	3-Methoxy Phenyl	H	>100
10	4-Methoxy Phenyl	H	>100
11	3-Chloro Phenyl	H	>100
12	4-Chloro Phenyl	H	>100
13	2-Methyl phenyl	H	>100
14	3-Methyl phenyl	H	>100
15	4-Methyl phenyl	H	>100
16	4-Ethyl phenyl	H	48.2
17	4-Nitro phenyl	H	>100
18	Phenyl-4-carboxylic acid	H	>100
19	1-Naphthyl	H	121.9
20	Phenyl ethyl	H	>100

molecules were manually analyzed to pick different scaffolds (Fig. 1) that makes a diverse set. Among the top 4-(5,7-dioxo-5H-pyrrolo[3,4-b]pyridin-6(7H)-yl)-2-fluorobenzenesulphonamide has created interest, because it has phthalimide (1,3-dioxoisindolin-2-yl) kind of scaffold bonded to sulphonamide group. Many sulphonamides were reported as protease inhibitor for HIV [25] and HCV [26]. Moreover, sulphonamides mimic peptide bond by increasing the stability towards protease catalyzed degradation [27]. Apart from it, phthalimide derivatives are reported to have antiviral activities [28], antimycobacterial activities [29] and they are very recently reported to have anticancer activity [30]. This created enthusiasm to synthesize few phthalimide–sulphonamides hybrid analogues. We synthesized few 4-(1,3-dioxoisindolin-2-yl) benzenesulphonamide derivatives (see Table 1) and investigated for anti DENV2 protease activity and two compounds were found to have DENV2 protease inhibitory activity at lower micro molar concentration. In order to understand the interaction of active compounds (16 and 19) with the DENV2 protease, protein structure was modelled against DENV3 X-ray crystal structure (PDB: 3U11). This has provided much clear picture of DENV2 protease in its catalytically competent form.

## 2. Experimental section

### 2.1. Materials and methods

Chemicals and solvents were of reagent grade and purchased from Sigma–Aldrich/Merck/CDH/Rankem. Completions of reaction were monitored on TLC plates (Merck™, KGaA, Germany). Melting

points were determined on an OPTIMELT automated system apparatus and are uncorrected melting points. Intermediate was characterized by its melting point. Final compounds were characterized by their  $^1\text{H}$  NMR (400 MHz) VNMRS 400, in  $\text{DMSO}-d_6$  as a solvent.  $^{13}\text{C}$  NMR was done in Bruker AMX 300 NMR spectrometer with tetra methyl silane as internal standard. Mass spectra were recorded by WATERS-Q-T of Premier-HAB213 using the (ESI-MS) Electro spray Ionization technique. In the Proton NMR Spectra the coupling constants ( $J$ ) are expressed in hertz (Hz). Chemical shifts ( $\delta$ ) of NMR are reported in parts per million (ppm) units relative to the solvent. For X-ray crystal structure, data collection was done using APEX2, cell refinement was done using APEX2, data reduction was done using SAINT, SHELXL97 program was used to solve and refine the structure, molecular graphics was done using ORTEP-3 and software used to prepare material for publication are SHELXL97 and PLATON. For computational analysis, a molecular docking study was performed using GLIDE, Schrodinger suite 2009. Molecular Dynamics simulation analysis was done using AMBER.

## 2.2. General procedure for 2-Phenyl-1, 3-isoindolinedione [31]

A mixture of aniline (0.36 mL, 4.0 mmol), phthalic anhydride (0.5 g, 3.4 mmol), and 20 mL of glacial acetic acid was stirred under nitrogen at 120 °C for 2 h. After that the mixture was cooled and 30 mL of cold water was added. A white colour product precipitated out. The product was filtered and washed with cold water and dried. Yield is 90%.

## 2.3. General procedure for 4-(1, 3-Dioxo-2, 3-dihydro-1H-2-isoindolyl)-1-benzenesulfonyl chloride [31]

To a solution of 0.16 g (0.09 mL, 1.35 mmol) of chlorosulphonic acid and 0.14 g (0.67 mmol) of phosphorus pentachloride that had been stirred for 10 min, was added 0.15 g (0.67 mmol) of N-phenyl-phthalimide in small portion. The resulting mixture was stirred and heated at 60 °C for 30 min. The reaction mixture was poured onto ice and extracted with chloroform. The organic phase was separated, washed with brine, dried over anhydrous sodium sulfate and evaporated *in vacuo* to furnish compound in 70% yield, as a white solid. Mp 180–182 °C.

## 2.4. Representative procedure for sulphonamides (1–20)

To a solution of sulphonyl chloride derivative (0.5 g, 1.56 mmol) in 50 mL of methylene chloride in round bottom flask kept under ice bath was added pyridine (1.872 mmol) and stirred for half an hour and to this mixture was added the functionalized amine derivatives (3.12 mmol). The reaction mixture was stirred for about 0.5–4 h, at room temperature. The reaction was monitored by TLC. Next, the phthalimide derivatives 1–20 were isolated by addition of 50 mL of methylene chloride and extraction with 1 N HCl and brine. The organic layer was dried over anhydrous sodium sulfate and evaporated *in vacuo* to give the sulphonamide derivatives in good to excellent yields.  $^1\text{H}$ NMR,  $^{13}\text{C}$ NMR, MS spectra of the compounds and addition X-ray crystal structure information are provided in [supplementary material](#).

### 2.4.1. 4-(1,3-Dioxoisindolin-2-yl)benzenesulphonamide (1)

Yield = 81%; Pale white amorphous powder. Mp: 320–322 °C;  $^1\text{H}$  NMR (400 MHz,  $\text{DMSO}-d_6$ )  $\delta$  7.46 (s, 1H, —NH), 7.67 (d, 2H,  $J = 8.4$  Hz, Ar—H), 7.96 (m, 4H, Ar—H); MS (ESI):  $m/z$  303 [M + H] $^+$ .

### 2.4.2. 4-(1,3-Dioxoisindolin-2-yl)-N,N-dimethyl benzenesulphonamide (2)

Yield = 85%; Pale white amorphous powder. Mp 242–244 °C;  $^1\text{H}$  NMR (400 MHz,  $\text{DMSO}-d_6$ )  $\delta$  2.15 (s, 3H, —CH<sub>3</sub>), 2.38 ((m, 4H,

—(CH<sub>2</sub>)—N), 2.94 (m, 4H, Ar), 7.78 (d, 2H,  $J = 8.4$  Hz, Ar—H), 7.88 (m, 4H, Ar—H), 8.00 (m, 2H, Ar—H); MS (ESI):  $m/z$  330 [M] $^+$ .

### 2.4.3. 4-(1,3-Dioxoisindolin-2-yl)-N,N-diethyl benzenesulphonamide (3)

Yield = 94%; Pale white amorphous powder. Mp: 178–180 °C;  $^1\text{H}$  NMR (400 MHz,  $\text{DMSO}-d_6$ )  $\delta$  1.08 (t, 6H, —(CH<sub>3</sub>),  $J = 6.8$  Hz), 3.21(q, 4H, —(CH<sub>2</sub>)—,  $J = 7.2$  Hz), 7.71(d, 2H,  $J = 8.4$  Hz, Ar—H), 7.96(m, 6H, Ar—H);  $^{13}\text{C}$ NMR (75 MHz,  $\text{DMSO}-d_6$ )  $\delta$  14.35, 42.13, 123.65, 127.45, 127.65, 131.48, 134.95, 135.54, 138.75, 166.62; MS (ESI):  $m/z$  359 [M + H] $^+$ .

### 2.4.4. 4-(1,3-Dioxoisindolin-2-yl)-N-isopropyl benzenesulphonamide (4)

Yield = 95%; Pale white amorphous powder. Mp: 188–190 °C;  $^1\text{H}$  NMR (400 MHz,  $\text{DMSO}-d_6$ )  $\delta$  0.98 (d, 6H, (CH<sub>3</sub>)<sub>2</sub>,  $J = 6.8$  Hz), 1.09(m, 1H, —CH), 7.73 (m, 4H, Ar—H), 7.96 (m, 6H, Ar—H); MS (ESI):  $m/z$  345 [M + H] $^+$ .

### 2.4.5. 2-(4-(Piperidin-1-ylsulphonyl)phenyl)isoindoline-1,3-dione (5)

Yield = 80%; Pale white amorphous powder. Mp: 165–167 °C;  $^1\text{H}$  NMR (400 MHz,  $\text{DMSO}-d_6$ )  $\delta$  2.59(s, 3H, —CH<sub>3</sub>), 2.68 (s, 3H, —CH<sub>3</sub>), 7.36 (d, 1H,  $J = 6.4$  Hz, Ar—H), 7.57(m, 1H, Ar—H), 7.76 (m, 2H, Ar—H), 7.97(m, 4H, Ar—H);  $^{13}\text{C}$ NMR (75 MHz,  $\text{DMSO}-d_6$ )  $\delta$  22.81, 24.75, 46.65, 123.65, 127.49, 128.17, 128.63, 131.46, 134.52, 134.95, 135.92, 166.57; MS (ESI):  $m/z$  371 [M + H] $^+$ .

### 2.4.6. 2-(4-(4-Methylpiperazin-1-ylsulphonyl)phenyl)isoindoline-1,3-dione (6)

Yield = 80%; Pale white amorphous powder. Mp: 191–193 °C;  $^1\text{H}$  NMR (400 MHz,  $\text{DMSO}-d_6$ )  $\delta$  1.56 (m, 4H, —(CH<sub>2</sub>)—NH), 2.95 ((m, 4H, —(CH<sub>2</sub>)—N), 7.76(m, 2H, Ar—H), 7.88 (m, 4H, Ar—H), 8.00 (m, 2H, Ar—H), 8.32(s, 1H, NH); MS (ESI):  $m/z$  386 [M + H] $^+$ .

### 2.4.7. 4-(1,3-Dioxoisindolin-2-yl)-N-phenylbenzenesulphonamide (7)

Yield = 68%; Off white amorphous powder (purified by column chromatography using hexane/ethyl acetate 1:1 as eluent). Mp 226–228 °C;  $^1\text{H}$  NMR (400 MHz,  $\text{DMSO}-d_6$ )  $\delta$  7.05 (t, 1H,  $J = 7.6$  Hz, Ar—H), 7.15 (d, 2H,  $J = 4$  Hz, Ar—H), 7.26(t, 2H,  $J = 7.6$  Hz, Ar—H), 7.67 (d, 2H, 8.4 Hz), 7.93 (m, 4H, Ar—H), 7.98(m, 2H, Ar—H), 10.42(s, 1H, NH); MS (ESI):  $m/z$  379 [M + H] $^+$ .

### 2.4.8. 4-(1,3-Dioxoisindolin-2-yl)-N-(2-hydroxyphenyl)benzenesulphonamide (8)

Yield: 86% Pale brownish white amorphous powder. Mp: 392–394 °C,  $^1\text{H}$  NMR ( $\text{DMSO}-D_6$ )  $\delta$  6.73 (m, 2H, Ar), 6.95 (m, 1H, Ar), 7.18 (d, 1H, Ar,  $J = 8.8$  Hz), 7.68 (m, 2H, Ar), 7.94 (m, 6H, Ar), 9.45 (s, 1H, NH), 9.7 (s, 1H, OH); MS (ESI):  $m/z$  394 [M] $^+$ .

### 2.4.9. 4-(1,3-Dioxoisindolin-2-yl)-N-(3-methoxyphenyl)benzenesulphonamide (9)

Yield: 85%; Pale white amorphous powder. Mp: 203–205 °C;  $^1\text{H}$  NMR (400 MHz,  $\text{DMSO}-d_6$ )  $\delta$  3.67 (s, 3H, OCH<sub>3</sub>), 6.71 (m, 2H, Ar—H), 7.15 (t, 1H,  $J = 8.4$  Hz, Ar—H), 7.6 (d, 2H,  $J = 8.4$  Hz, Ar—H), 7.92 (m, 4H, Ar—H), 7.98 (m, 2H, Ar—H), 10.42 (s, 1H, NH); MS (ESI):  $m/z$  409 [M + H] $^+$ .

### 2.4.10. 4-(1,3-Dioxoisindolin-2-yl)-N-(4-methoxyphenyl)benzenesulphonamide (10)

Yield: 79%; Pale white amorphous powder. Mp: 168–170 °C;  $^1\text{H}$  NMR (400 MHz,  $\text{DMSO}-d_6$ )  $\delta$  3.67 (s, 3H, OCH<sub>3</sub>), 6.83 (d, 2H,  $J = 9.2$  Hz, Ar—H), 7.03 (d, 2H,  $J = 8.8$  Hz, Ar—H), 7.16 (m, 1H, Ar—H), 7.25 (m, 1H, Ar—H), 7.65(d, 2H,  $J = 8.8$  Hz, Ar—H), 7.84(d, 2H,  $J = 8.8$  Hz, Ar—H), 7.92 (m, 2H, Ar—H), 7.98 (m, 2H, Ar—H), 10.05(s, 1H, NH); MS (ESI):  $m/z$  409 [M + H] $^+$ .

2.4.11. *N*-(3-chlorophenyl)-4-(1,3-dioxoisindolin-2-yl)benzenesulphonamide (11)

Yield: 81%; Buff white amorphous powder. Mp: 223–225 °C; <sup>1</sup>H NMR (400 MHz, DMSO-*d*<sub>6</sub>) δ 7.140 (t, 2H, *J* = 8 Hz, Ar–H), 7.172 (s, 1H, Ar–H), 7.30 (t, 1H, *J* = 7.6 Hz, Ar–H), 7.70 (d, 2H, *J* = 8.4 Hz, Ar–H), 7.91 (m, 2H, Ar–H), 7.93 (m, 2H, Ar–H), 7.98 (m, 2H, Ar–H), 10.7 (s, 1H, NH); MS (ESI): *m/z* 412 [M]<sup>+</sup>.

2.4.12. *N*-(4-chlorophenyl)-4-(1,3-dioxoisindolin-2-yl)benzenesulphonamide (12)

Yield: 83%; Pale white amorphous powder. Mp: 212–214 °C; <sup>1</sup>H NMR (400 MHz, DMSO-*d*<sub>6</sub>) δ 7.16 (d, 2H, *J* = 9.2 Hz, Ar–H), 7.32 (d, 2H, *J* = 8.8 Hz, Ar–H), 7.68 (d, 2H, *J* = 8 Hz, Ar–H), 7.92 (m, 4H, Ar–H), 7.99 (m, 2H, Ar–H), 10.57 (s, 1H, NH); MS (ESI): *m/z* 412 [M]<sup>+</sup>.

2.4.13. 4-(1,3-Dioxoisindolin-2-yl)-*N*-*o*-tolylbenzenesulphonamide (13)

Yield: 89%. Pale pink amorphous powder. Mp: 391–393 °C, <sup>1</sup>H NMR (DMSO-*D*<sub>6</sub>) δ 2.03 (s, 3H, CH<sub>3</sub>), 7.01 (m, 1H, Ar), 7.14 (m, 3H, Ar), 7.67 (d, 2H, Ar, *J* = 8.4 Hz), 7.82 (d, 2H, Ar, *J* = 8.8 Hz), 7.92 (m, 2H, Ar), 7.99 (m, 2H, Ar), 9.72 (s, 1H, NH); MS (ESI): (*m/z*) 393 [M + H]<sup>+</sup>.

2.4.14. 4-(1,3-Dioxoisindolin-2-yl)-*N*-*m*-tolylbenzenesulphonamide (14)

Yield = 90%; Pale pinkish white amorphous powder. Mp: 241–243 °C; <sup>1</sup>H NMR (400 MHz, DMSO-*d*<sub>6</sub>) δ 2.21 (s, 3H, CH<sub>3</sub>), 6.86 (d, 1H, *J* = 7.2 Hz, Ar–H), 6.95 (d, 2H, *J* = 6.8 Hz, Ar–H), 7.13 (t, 1H, *J* = 8 Hz, Ar–H), 7.66 (d, 2H, *J* = 8.8 Hz, Ar–H), 7.91 (m, 4H, Ar–H), 7.98 (m, 2H, Ar–H), 10.33 (s, 1H, NH); MS (ESI): *m/z* 393 [M + H]<sup>+</sup>.

2.4.15. 4-(1,3-Dioxoisindolin-2-yl)-*N*-*p*-tolylbenzenesulphonamide (15)

Yield = 84%; Off white amorphous powder. Mp: 224–226 °C; <sup>1</sup>H NMR (400 MHz, DMSO-*d*<sub>6</sub>) δ 2.19 (s, 3H, CH<sub>3</sub>), 7.04 (dd, 4H, *J* = 13.2 Hz, 8.8 Hz, Ar–H), 7.65 (d, 2H, *J* = 8 Hz, Ar–H), 7.91 (m, 4H, Ar–H), 7.98 (m, 2H, Ar–H), 10.24 (s, 1H, NH); MS (ESI): *m/z* 393 [M + H]<sup>+</sup>.

2.4.16. 4-(1,3-Dioxoisindolin-2-yl)-*N*-(4-ethylphenyl)benzenesulphonamide (16)

Yield = 88%; Pale pinkish white amorphous powder. Mp 212–214 °C; <sup>1</sup>H NMR (400 MHz, DMSO-*d*<sub>6</sub>) δ 1.19 (t, 3H, –CH<sub>3</sub>, *J* = 7.2 Hz), 2.59 (q, 2H, –CH<sub>2</sub>–, *J* = 7.4 Hz), 7.01 (d, 2H, *J* = 8.4 Hz, Ar–H), 7.09 (d, 2H, *J* = 8.0 Hz, Ar–H), 7.63 (d, 2H, *J* = 8.4 Hz, Ar–H), 7.84 (m, 4H, Ar–H), 7.96 (m, 4H, Ar–H); <sup>13</sup>CNMR (75 MHz, DMSO-*d*<sub>6</sub>) δ 15.45, 27.46, 120.43, 123.66, 127.40, 127.52, 128.56, 131.44, 134.96, 135.11, 135.68, 138.64, 139.80, 166.56; MS (ESI): *m/z* 406 [M]<sup>+</sup>.

2.4.17. 4-(1,3-Dioxoisindolin-2-yl)-*N*-(4-nitrophenyl)benzenesulphonamide (17)

Yield = 75%; Pale yellow colour amorphous powder. Mp: 244–246 °C; <sup>1</sup>H NMR (400 MHz, DMSO-*d*<sub>6</sub>) δ 7.37 (d, 2H, *J* = 9.2 Hz, Ar–H), 7.72 (d, 2H, *J* = 8.8 Hz, Ar–H), 7.91 (d, 2H, *J* = 3.2 Hz, Ar–H), 7.98 (d, 2H, *J* = 3.2 Hz, Ar–H), 8.05 (d, 2H, *J* = 8.4 Hz, Ar–H), 8.17 (d, 2H, *J* = 9.2 Hz, Ar–H), 11.43 (s, 1H, NH); MS (ESI): *m/z* 423 [M]<sup>+</sup>.

2.4.18. 4-(4-(1,3-Dioxoisindolin-2-yl)phenylsulphonamido)benzoic acid (18)

Yield = 76%; Pale pinkish white amorphous powder. Mp: 263–265 °C; <sup>1</sup>H NMR (400 MHz, DMSO-*d*<sub>6</sub>) δ 7.26 (d, 2H, *J* = 8.4 Hz, Ar–H), 7.70 (d, 2H, *J* = 9.2 Hz, Ar–H), 7.83 (d, 2H, *J* = 8.8 Hz,

Ar–H), 7.91 (m, 2H, Ar–H), 8.02 (m, 4H, Ar–H), 10.94 (s, 1H, NH); <sup>13</sup>CNMR (75 MHz, DMSO-*d*<sub>6</sub>) δ 118.19, 123.67, 125.81, 126.15, 126.76, 127.29, 127.50, 127.64, 130.91, 131.43, 134.96, 136.08, 138.25, 141.89, 142.07, 146.28, 166.50, 166.79; MS (ESI): *m/z* 423 [M + H]<sup>+</sup>.

2.4.19. 4-(1,3-Dioxoisindolin-2-yl)-*N*-(naphthalen-1-yl)benzenesulphonamide (19)

Yield = 88%; Pale purple colour amorphous powder. Mp: 198–200 °C; <sup>1</sup>H NMR (400 MHz, DMSO-*d*<sub>6</sub>) δ 7.21 (d, 1H, *J* = 8 Hz, Ar–H), 7.40–7.50 (m, 3H, Ar–H), 7.62 (s, 1H, Ar–H), 7.64 (s, 1H, Ar–H), 7.86 (d, 1H, *J* = 8 Hz, Ar–H), 7.89–7.99 (m, 7H, Ar–H), 8.04 (d, 1H, *J* = 8 Hz, Ar–H), 10.37 (s, 1H, NH); MS (ESI): *m/z* 429 [M + H]<sup>+</sup>.

2.4.20. 4-(1,3-Dioxoisindolin-2-yl)-*N*-phenethylbenzenesulphonamide (20)

Yield = 90%; Pale white amorphous powder. Mp: 170–172 °C; <sup>1</sup>H NMR (400 MHz, DMSO-*d*<sub>6</sub>) δ 2.78 (m, 2H, –CH<sub>2</sub>–), 3.03 (m, 2H, –CH<sub>2</sub>–), 7.27 (m, 5H, Ar–H), 7.62 (m, 3H, Ar–H), 7.76 (s, 1H, Ar–H), 7.91 (m, 5H, Ar–H), 10.72 (s, 1H, NH); <sup>13</sup>CNMR (75 MHz, DMSO-*d*<sub>6</sub>) δ 35.38, 44.18, 123.66, 126.33, 127.25, 127.66, 128.40, 128.75, 131.52, 134.95, 135.34, 138.69, 139.54, 166.66; MS (ESI): *m/z* 407 [M + H]<sup>+</sup>.

2.5. X-ray crystallographic study of Compound **16**

Single crystals of compound **16** suitable for X-ray diffraction were obtained by slow evaporation method. Three dimensional intensity data were collected on a Bruker SMART APEX CCD [32] diffractometer using graphite monochromatized Mo K $\alpha$  radiation ( $\lambda$  = 0.71073 Å). The intensity data collection, frames integration, Lorentz Polarization (LP) correction were done using SAINT software [32]. Empirical absorption correction (multi-scan) was performed using SADABS program [32]. The structure was solved by direct methods using SHLEXS 97 and refined by full-matrix least-squares procedures using SHELXL97 programs [33]. The molecular geometry was calculated using PARST [32]. All non-hydrogen atoms were first refined isotropically and then with anisotropic displacement parameters. The hydrogen atoms were included in the structure factor calculation at idealized positions by using a riding model, but not refined. The final *R*-factor converged to 4.3%. Table 2 summarizes the crystal data. Compound **16**, C<sub>22</sub>H<sub>18</sub>N<sub>2</sub>O<sub>4</sub>S<sub>1</sub> crystallizes in monoclinic P 2<sub>1</sub>/c space group. The ORTEP plot [34] of the molecule is shown in Fig. 2. The isoindole ring adopts a planar conformation and cyclobenzene rings (C9–C14) and (C15–C20) also adopt a planar conformation. The isoindole ring makes a dihedral angle of 48.16 (1)° with the cyclobenzene ring (C9–C14) and 84.28 (1)° with the cyclobenzene ring (C15–C20).

In the crystal, the molecular structure is stabilized by intermolecular of N–H...O hydrogen bonds, generating the R<sub>2</sub><sup>2</sup> (8) ring motifs [35] and intramolecular C–H...O hydrogen bonds. (Fig. 3 and Table 3). Selected bond lengths and bond angles are given in supplementary information.

2.6. DENV2 protease assay [36]

To measure the inhibitory activities of the compounds, the DENV2 NS2B–NS3 protease activities were measured in the presence of the compounds using Bz-Nle-Lys-Arg-Arg-AMC as a substrate. The enzyme concentration in the assay was 125 nM, and the substrate concentration was 20 μM in 10 mM Tris–HCl pH 8.5, 20% Glycerol, and 1 mM CHAPS. The inhibitor concentrations were 100 μM for the first round and between 3.125 and 400 μM for the compounds **16** and **19** in the second round. Before adding

**Table 2**  
Summary of crystallographic data collection and refinement data.

Molecular formula	$C_{22}H_{18}N_2O_4S$	$F(000)$	848
Cell volume	1947.87 (7)	Crystal size (mm)	$0.30 \times 0.25 \times 0.20$
Unit cell parameters (Å)	$a = 11.8320(2)$ $b = 8.3022(2)$ $c = 20.6777(4)$ $\beta = 106.473(4)$	Theta range for data collection (°)	1.8–28.40
Crystal system	Monoclinic	Limiting indices	$-15 \leq h \leq 15$ $-11 \leq k \leq 11$ $-27 \leq l \leq 27$
Space group	$P2_1/c$	Reflections collected/unique	18,290/4844
Mol. weight	406.44	Refinement method	Full-matrix least-squares on $F^2$
Z, Dcal (mg m <sup>-3</sup> )	4, 1.386	Data/restraints/parameters	4844/0/263
Crystal Habit	Block	Goodness-of-fit on $F^2$	1.050
Crystal Colour	Colourless	Final R indices [ $I > 2\sigma(I)$ ]	$R1 = 0.043$ $WR2 = 0.111$
R-factor	0.043	R indices (all data)	$R1 = 0.072$ $WR2 = 0.125$
Abs. Coeff	0.031	Largest diff. peak and hole (e Å <sup>-3</sup> )	0.039 and -0.39

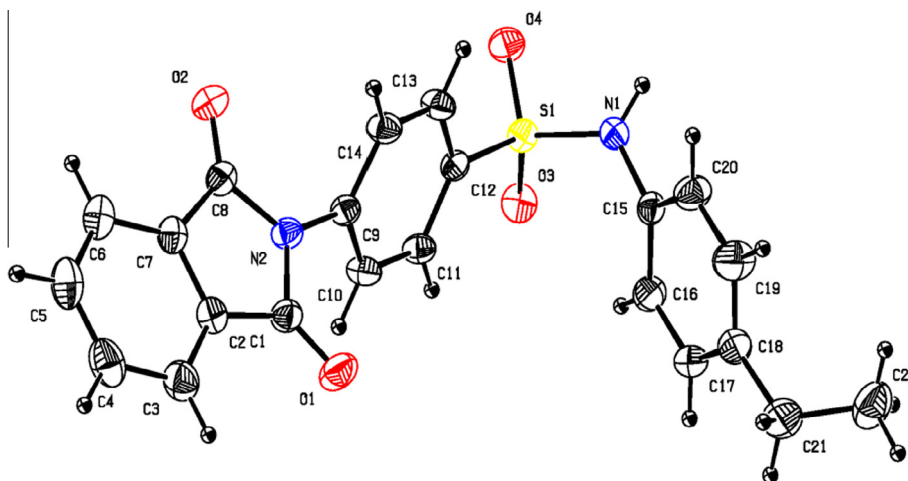


**Fig. 2.** ORTEP diagram of compound **16**. Displacement ellipsoids are drawn at 30% probability level.

the substrate, the enzyme and the inhibitors were incubated at 37 °C for 15 min. All inhibition measurements were carried out in three independent determinations which were performed in duplicate and the experimental values were averaged. All reactions were performed in 96-well plates with a final volume of 50  $\mu$ L per each wells using the FLx800 fluorescence micro plate reader (BioTek) with excitation wavelength at 380 nm, and emission wavelength at 460 nm.  $IC_{50}$  values were determined using GraphPad Prism 5.0 (GraphPad Software).

### 2.7. Molecular docking

To investigate mechanism of action, docking studies were performed for two active compounds. The FASTA sequence of dengue virus NS2B–NS3 protease (PDB code: 2FOM [24]) was downloaded from [www.rcsb.org](http://www.rcsb.org) was modelled from 3U1I [40] as template using Modeller 9.15. To understand the binding pattern of active compounds with NS2B–NS3 Protease, induced fit docking was performed by molecular modelling software GLIDE of Maestro 9.2, Schrodinger suite 2009 [37].

Glide calculations use an all-atom force field for accurate energy evaluation. Thus, Glide requires bond orders and ionization states to be properly assigned and performs better when side chains are reoriented when necessary and steric clashes are relieved. A

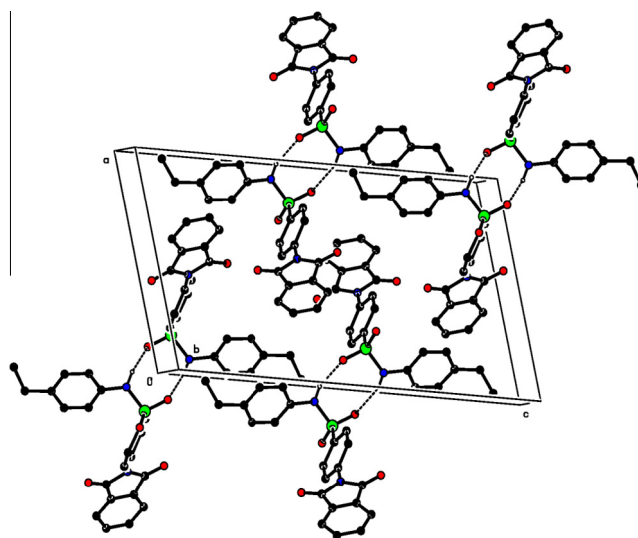


**Fig. 3.** The crystal packing of the compound **16** viewed along the  $b$  axis. The hydrogen bonds are shown as dashed lines (see supplementary information for details; H-atoms not involved in H-bonds have been excluded for clarity).

**Table 3**  
Hydrogen-bond geometry (Å) for compound **14**.

D—H...A	D—H (Å)	H...A (Å)	D...A (Å)	D—H...A [°]
N(1)—H(1)...O(4) <sup>i</sup>	0.86	2.33	2.943(2)	128
C(11)—H(11)...O(3)	0.97	2.52	2.893(2)	104
C(16)—H(16)...O(3)	0.93	2.47	3.084(2)	124

Symmetry codes:  $i = -x + 2, -y + 2, -z + 2$ .

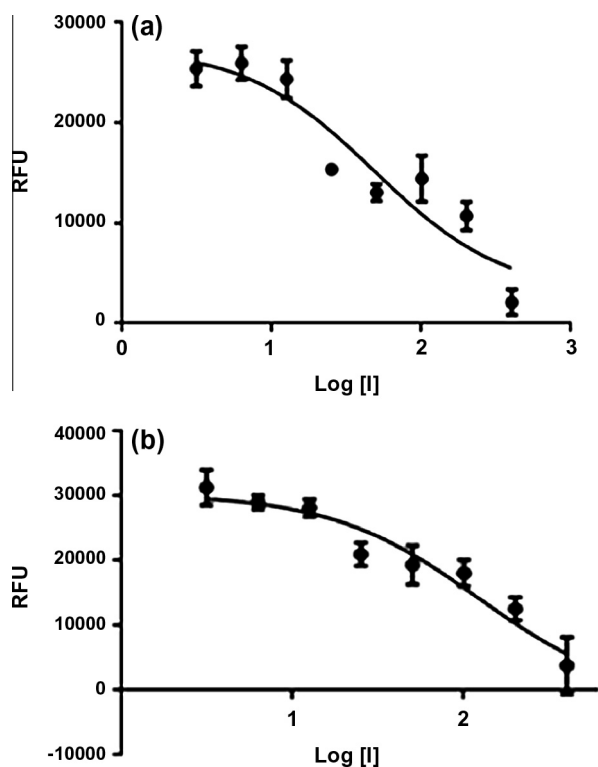
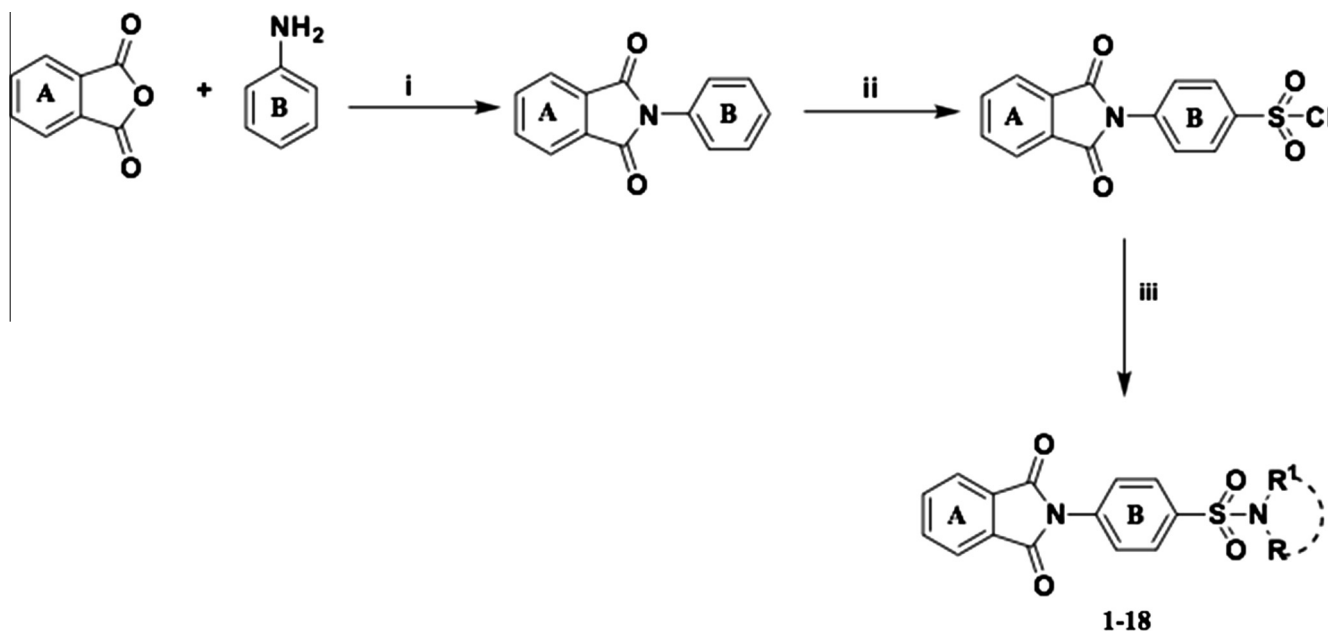


Fig. 4. (a) IC<sub>50</sub> of compound **16**; (b) IC<sub>50</sub> of compound **19**.



**Scheme 1.** Reagents and conditions: (i) Glacial acetic acid, reflux, 4 h (ii) PCl<sub>5</sub>, HSO<sub>3</sub>Cl, DCM, 0 °C-rt and reflux, 0.5 h (iii) various anilines/amines as shown in Table 1, Pyridine, DCM, 0 °C-rt, 0.5–5 h.

grid was constructed around the active site residues His90, Asp114 and Ser174 using receptor grid generation protocol of Maestro 9.2 module Schrodinger suite 2009.. The structure of compounds **16** and **19** were sketched using build panel and prepared for docking using Ligprep module in Maestro 9.2 (Schrodinger LLC). Ligands were minimized using OPLS\_2005 force field, while all the other parameter were kept unaltered.

The ligands were docked with the constructed grid using the 'Extra precision' Glide algorithm [38]. Glide uses a hierarchical series of filters to search for possible locations of the ligand in the active-site region of the receptor. Final scoring of docked ligand is carried out on the energy-minimized poses Glide Score scoring function.

### 3. Results and discussion

#### 3.1. Chemistry

All the compounds were synthesized through reactions outlined in Scheme 1. The intermediate 4-(1,3-dioxisoindolin-2-yl)benzene-1-sulphonyl chloride was synthesized from 2-phenylisoindoline-1,3-dione by chlorosulphonation reaction [39]. The second step involves S<sub>N</sub><sup>2</sup> nucleophilic substitution of chloride in the intermediate with amino group of amines/aniline derivatives. The hydrochloric acid liberated was trapped with the base pyridine which favours the forward reaction that provided compounds **1–20** as shown in Table 1. Intermediate was characterized by its melting point (Lit. value 180–182 °C [39]). All the final compounds were characterized by their <sup>1</sup>HNMR, <sup>13</sup>CNMR and MS analysis. In <sup>1</sup>HNMR, the proton of sulphomoyl —NH displayed a characteristic singlet between δ 9.45 and δ 11.43 ppm (except compound **2**, **3**, **5** and **6**). A multiplet was obtained for the protons of ring A (isoindoline group) in the range of δ 7.84–8.02 ppm. Two multiplets were obtained for proton of ring B, one at around δ 7.57–7.76 ppm while the other at around δ 7.98–8.02 ppm. In <sup>13</sup>CNMR, all the aromatic carbons were in the range of δ 117–150 ppm and aliphatic carbons less than δ 50 ppm. Carboxylic acid group in compound **18** showed signal at δ 166 ppm. Primary carbons in compounds **3** and **16** gave signal

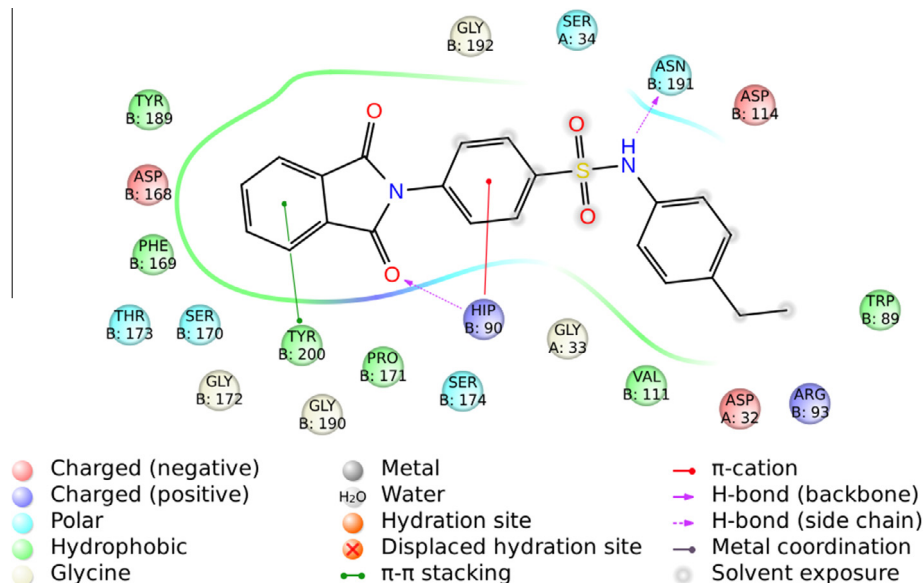


Fig. 5. 2-D plot showing interaction of compound **16** with modelled DENV2 NS2B/NS3 protease (figure generated using Maestro 9.2).

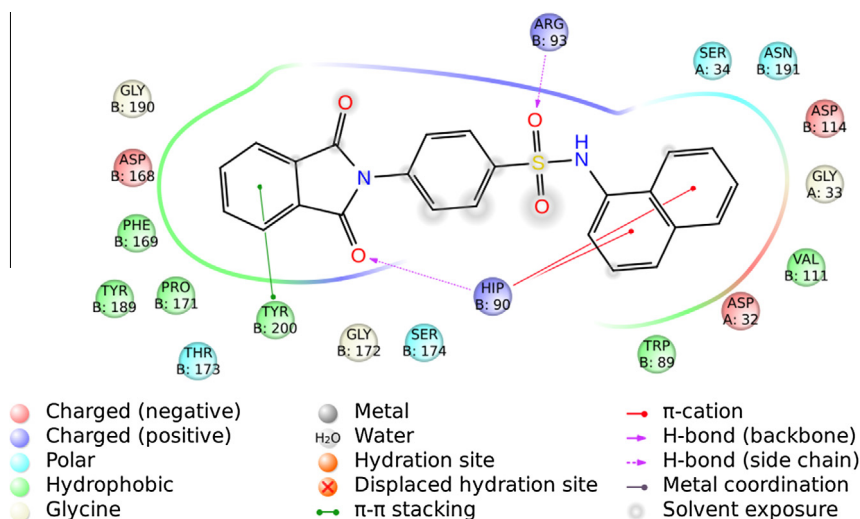


Fig. 6. 2-D plot showing interaction of compound **19** with modelled DENV2 NS2B/NS3 protease (figure generated using Maestro 9.2).

at  $\delta$  14–16 ppm confirmed by DEPT studies. Secondary carbons in compounds **3**, **5**, **14** and **16** showed  $\delta$  at 22–47 ppm which were confirmed by negative peak in DEPT-135. Tertiary carbons in compounds **3**, **5**, **18** and **20** showed  $\delta$  at 118–136 ppm which were confirmed by positive peaks in DEPT-90. Whereas, quaternary carbons in compounds **3**, **5**, **16**, **18** and **20** showed  $\delta$  at 136–167 ppm, confirmed by absence of peak in DEPT-135. Mass spectra of all the compounds displayed an  $M^+/[M+H]^+$  as a base peak. Further, We have succeeded in obtaining a crystal of 4-(1, 3-dioxoisindolin-2-yl)-N-(4-ethylphenyl)benzenesulphonamide by slow evaporation of its ethanolic solution at room temperature and its X-ray crystallographic structure (Fig. 2) was determined through single crystal X-ray diffraction studies.

### 3.2. DENV Protease assay

All the twenty compounds were tested for their inhibitory activity against DENV2 NS2B–NS3 protease and the results are given in Table 1. Two compounds were found to be active (**16** and **19**) at the concentration of 100  $\mu$ M, all the other compounds

were found inactive. Activity at a serial dilution ranging from 3.125 to 400  $\mu$ M were performed for the active compounds, which gave  $IC_{50}$  value of 48.2  $\mu$ M for compound **16** and  $IC_{50}$  value of 121.9  $\mu$ M for compound **19** (Fig. 4a and b).

### 3.3. Molecular docking

Molecular docking of the compounds **16** and **19** have given a docking score of  $-5.12$  and  $-3.94$  respectively with the modelled DENV2 protease. The common interactions of both the active compounds (compound **16** and compound **19**) are given below (see Figs. 5 and 6).

- $\pi$  electron cloud of ring A interacts with  $\pi$  electron cloud of Tyr200 by  $\pi$ - $\pi$  stacking interaction.
- Oxygen atom present in carbonyl group of ring A, interacts with nitrogen atom present in imidazole group of Hip90 to have H-bond with a distance of 3.05 Å and 2.95 Å for the compounds **16** and **19** respectively.

- =CH group present in ring A interacts with residues Asp168, Phe169, Pro171, Tyr189 and Gly190 with hydrophobic interactions.
- 4-ethyl phenyl group attached to sulphonamide in compound **16** and naphthyl group attached to sulphonamide in compound **19** have hydrophobic interactions with residues Trp89 and Val111.

As there is difference in size, shape and volume of both the active ligands, their interaction pattern in molecular docking with modelled DENV2 protease differs. Specific interactions of Compound **16** are given below.

- Nitrogen atom present in sulphonamide group interacts with oxygen atom present in side chain carbonyl group of Asn191 with H-bond having a distance of 3.08 Å.
- $\pi$  electron cloud of ring B and cationic nitrogen species present in imidazole ring of Hip90 interacts with  $\pi$ -cation interaction.

Compound **19** contain a bulkier naphthyl group, which made some specific interactions in molecular docking with modeled DENV2 protease given below.

- Oxygen atom of sulphonamide group, which is at 2.75 Å distance to —NH group of side chain of residue Arg93 interacts with H-bond.
- $\pi$  electron cloud present in bulkier naphthyl group and cationic nitrogen species present in imidazole ring of Hip90 interacts with  $\pi$ -cation interaction.

Based on foregoing discussion, it can be concluded that the  $\pi$ - $\pi$  stacking interactions, hydrogen bond interactions, hydrophobic interactions,  $\pi$ -cation interactions of the active ligands with the above discussed residues are important for activity and potency of the inhibitors.

## Acknowledgments

Author is thankful to Department of Biotechnology (Govt. of India) for providing financial support through one of its INDO-GERMAN project (BT/IN/GERMAN/15/DV/2010), Linlin Zhang of University of Leubeck and German Center for Infection Research (DZIF), Germany for IC<sub>50</sub> of DENV protease assay studies to complete this manuscript. Authors are also thankful to Dr. Reddy's Institute of Life Science, Hyderabad for NMR and Mass spectral studies.

## Appendix A. Supplementary material

CCDC 1030907 contains the supplementary crystallographic data of Compound **16**. This data can be obtained free of charge from the Cambridge Crystallographic Centre via [www.ccdc.cam.ac.uk/data\\_request/cif](http://www.ccdc.cam.ac.uk/data_request/cif). Supplementary data associated with this article can be found, in the online version, at <http://dx.doi.org/10.1016/j.bioorg.2015.07.005>.

## References

- [1] P. Lai, S. Lee, C. Kao, Y. Chen, C. Huang, W. Lin, S. Wann, H. Lin, M. Yen, Y. Liu, Characteristics of a dengue hemorrhagic fever outbreak in 2001 in Kaohsiung, J. Microbiol. Immunol. Infect. 37 (2004) 266.
- [2] S.H. Waterman, D.J. Gubler, Dengue fever, Clin. Dermatol. 7 (1989) 117–122.
- [3] W.H. Organization, Dengue Prevention and Control, DOI, 2002.
- [4] D.J. Gubler, G.G. Clark, Dengue/dengue hemorrhagic fever: the emergence of a global health problem, Emerg. Infect. Dis. 1 (1995) 55.
- [5] J.G. Rigau-Pérez, G.G. Clark, D.J. Gubler, P. Reiter, E.J. Sanders, A.V. Vorndam, Dengue and dengue haemorrhagic fever, The Lancet 352 (1998) 971–977.
- [6] E.A. Henchal, J.R. Putnak, The dengue viruses, Clin. Microbiol. Rev. 3 (1990) 376–396.
- [7] W.H. Organization, Dengue and severe dengue, Fact sheet N 117, WHO, DOI, Geneva, 2012.
- [8] S. Bhatt, P.W. Gething, O.J. Brady, J.P. Messina, A.W. Farlow, C.L. Moyes, J.M. Drake, J.S. Brownstein, A.G. Hoen, O. Sankoh, The global distribution and burden of dengue, Nature 496 (2013) 504–507.
- [9] O.J. Brady, P.W. Gething, S. Bhatt, J.P. Messina, J.S. Brownstein, A.G. Hoen, C.L. Moyes, A.W. Farlow, T.W. Scott, S.I. Hay, Refining the global spatial limits of dengue virus transmission by evidence-based consensus, PLoS Neglect. Trop. Dis. 6 (2012) e1760.
- [10] E.C. Holmes, S.S. Burch, The causes and consequences of genetic variation in dengue virus, Trends Microbiol. 8 (2000) 74–77.
- [11] K.V. Pugachev, F. Guirakhoo, D.W. Trent, T.P. Monath, Traditional and novel approaches to flavivirus vaccines, Int. J. Parasitol. 33 (2003) 567–582.
- [12] D.M. Andrews, H.M. Chaignot, B.A. Coomber, M.D. Dowle, S.L. Hind, M.R. Johnson, P.S. Jones, G. Mills, A. Patikis, T.J. Pateman, The design of potent, non-peptidic inhibitors of hepatitis C protease, Eur. J. Med. Chem. 38 (2003) 339–343.
- [13] R. Schober, R. Stehle, H. Walter, Tipranavir analogous 3-sulfonylanilidotronic acids: new synthesis and structure-dependent anti-HIV activity, Tetrahedron 64 (2008) 9401–9407.
- [14] B. Luna, U.T. Mary, Tipranavir: the first nonpeptidic protease inhibitor for the treatment of protease resistance, Clin. Ther. 29 (2007) 2309–2318.
- [15] L. de la Cruz, T.H.D. Nguyen, K. Ozawa, J. Shin, B. Graham, T. Huber, G. Otting, Binding of low molecular weight inhibitors promotes large conformational changes in the dengue virus NS2B–NS3 protease: fold analysis by pseudoccontact shifts, J. Am. Chem. Soc. 133 (2011) 19205–19215.
- [16] H. Lai, G.S. Prasad, R. Padmanabhan, Characterization of 8-hydroxyquinoline derivatives containing aminobenzothiazole as inhibitors of dengue virus type 2 protease in vitro, Antiviral Res. 97 (2013) 74–80.
- [17] S.M. Tomlinson, S.J. Watowich, Anthracene-based inhibitors of dengue virus NS2B–NS3 protease, Antiviral Res. 89 (2011) 127–135.
- [18] C. Steuer, C. Gege, W. Fischl, K.H. Heinonen, R. Bartenschlager, C.D. Klein, Synthesis and biological evaluation of  $\alpha$ -ketoamides as inhibitors of the Dengue virus protease with antiviral activity in cell-culture, Bioorg. Med. Chem. 19 (2011) 4067–4074.
- [19] C. Nitsche, C. Steuer, C.D. Klein, Arylcycanoacrylamides as inhibitors of the Dengue and West Nile virus proteases, Bioorg. Med. Chem. 19 (2011) 7318–7337.
- [20] H. Lai, D. Dou, S. Aravapalli, T. Teramoto, G.H. Lushington, T.M. Mwanja, K.R. Alliston, D.M. Eichhorn, R. Padmanabhan, W.C. Groutas, Design, synthesis and characterization of novel 1,2-benzisothiazol-3 (2H)-one and 1, 3, 4-oxadiazole hybrid derivatives: potent inhibitors of Dengue and West Nile virus NS2B/NS3 proteases, Bioorg. Med. Chem. 21 (2013) 102–113.
- [21] K.-C. Tiew, D. Dou, T. Teramoto, H. Lai, K.R. Alliston, G.H. Lushington, R. Padmanabhan, W.C. Groutas, Inhibition of Dengue virus and West Nile virus proteases by click chemistry-derived benz [d] isothiazol-3 (2H)-one derivatives, Bioorg. Med. Chem. 20 (2012) 1213–1221.
- [22] T.S. Kiat, R. Phippen, R. Yusof, H. Ibrahim, N. Khalid, N.A. Rahman, Inhibitory activity of cyclohexenyl chalcone derivatives and flavonoids of fingerroot, Boesenbergia rotunda (L.), towards dengue-2 virus NS3 protease, Bioorg. Med. Chem. Lett. 16 (2006) 3337–3340.
- [23] P. Badrinarayan, G. Narahari Sastry, Virtual high throughput screening in new lead identification, Comb. Chem. High throughput Screen. 14 (2011) 840–860.
- [24] P. Erbel, N. Schiering, A. D'Arcy, M. Renatus, M. Kroemer, S.P. Lim, Z. Yin, T.H. Keller, S.G. Vasudevan, U. Hommel, Structural basis for the activation of flaviviral NS3 proteases from dengue and West Nile virus, Nat. Struct. Mol. Biol. 13 (2006) 372–373.
- [25] G. Berube, A. Bouzide, A. Cote, G. Sauve, P. Soucy, B.R. Stranix, J. Yelle, Y. Zhao, Hiv protease inhibitors based on amino acid derivatives, Google Patents, 2002.
- [26] A.K. Lampa, S.M. Bergman, S.S. Gustafsson, H. Alogheli, E.B. Åkerblom, G.G. Lindeberg, R.M. Svensson, P. Artursson, U.H. Danielson, A. Karlén, Novel Peptidomimetic Hepatitis C Virus NS3/4A protease inhibitors spanning the P2–P1' region, ACS Med. Chem. Lett. 5 (2013) 249–254.
- [27] D.B. de Bont, K.M. Sliedregt-Bol, L.J. Hofmeyer, R.M. Liskamp, Increased stability of peptidylsulfonamide peptidomimetics towards protease catalyzed degradation, Bioorg. Med. Chem. 7 (1999) 1043–1047.
- [28] P. Selvam, D.R. Lakra, C. Pannecouque, E. De Clercq, Synthesis, antiviral and cytotoxicity studies of novel N-substituted indophenazine derivatives, Indian J. Pharm. Sci. 74 (2012) 275.
- [29] H. Akgün, I. Karamelekoğlu, B. Berk, I. Kurnaz, G. Sarıbiyık, S. Öktem, T. Kocagöz, Synthesis and antimycobacterial activity of some phthalimide derivatives, Bioorg. Med. Chem. 20 (2012) 4149–4154.
- [30] M. Matsushita, Y. Ozaki, Y. Hasegawa, F. Terada, N. Tabata, H. Shiheido, H. Yanagawa, T. Oikawa, K. Matsuo, W. Du, A novel Phthalimide derivative, TC11, has preclinical effects on high-risk myeloma cells and osteoclasts, PLoS One 10 (2015) e0116135.
- [31] L.d.M. Lima, P. Castro, A.L. Machado, C.A.M. Fraga, C. Lugnier, V.L.G. de Moraes, E.J. Barreiro, Synthesis and anti-inflammatory activity of phthalimide derivatives, designed as new thalidomide analogues, Bioorg. Med. Chem. 10 (2002) 3067–3073.
- [32] B. APEX, Bruker AXS Inc, Madison, WI, DOI, 2008.
- [33] G. Sheldrick, SADABS, v. 2008/1, Program for Empirical Absorption Correction of Area Detector Data, University of Göttingen, Göttingen, Germany, DOI, 2008.

- [34] L.J. Farrugia, WinGX and ORTEP for Windows: an update, *Appl. Crystallogr.* 45 (2012) 849–854.
- [35] J. Bernstein, R.E. Davis, L. Shimoni, N.L. Chang, Patterns in hydrogen bonding: functionality and graph set analysis in crystals, *Angew. Chem. Int. Ed. English* 34 (1995) 1555–1573.
- [36] C. Steuer, K.H. Heinonen, L. Kattner, C.D. Klein, Optimization of assay conditions for dengue virus protease: effect of various polyols and nonionic detergents, *J. Biomol. Screen.* 14 (2009) 1102–1108.
- [37] T.A. Halgren, R.B. Murphy, R.A. Friesner, H.S. Beard, L.L. Frye, W.T. Pollard, J.L. Banks, Glide: a new approach for rapid, accurate docking and scoring. 2. Enrichment factors in database screening, *J. Med. Chem.* 47 (2004) 1750–1759.
- [38] R.A. Friesner, R.B. Murphy, M.P. Repasky, L.L. Frye, J.R. Greenwood, T.A. Halgren, P.C. Sanschagrin, D.T. Mainz, Extra precision glide: docking and scoring incorporating a model of hydrophobic enclosure for protein-ligand complexes, *J. Med. Chem.* 49 (2006) 6177–6196.
- [39] W. Wang, W.A. Lim, A. Jakalian, J. Wang, J. Wang, R. Luo, C.I. Bayly, P.A. Kollman, An analysis of the interactions between the Sem-5 SH3 domain and its ligands using molecular dynamics, free energy calculations, and sequence analysis, *J. Am. Chem. Soc.* 123 (2001) 3986–3994.
- [40] C.G. Noble, C.C. Seh, A.T. Chao, P.Y. Shi, Ligand-bound structures of the dengue virus protease reveal the active conformation, *J. Virol.* 86 (2012) 438–446.